



1 Analysing Uncertainties in Offshore Wind Farm Power Output using 2 Measure Correlate Predict Methodologies.

3 Michael Denis Mifsud¹, Tonio Sant², Robert Nicholas Farrugia¹

4 ¹Institute for Sustainable Energy, University of Malta, Marsaxlokk, MXK1351 Malta.

5 ²Department of Mechanical Engineering, University of Malta, Msida, MSD2080, Malta.

6 *Correspondence to:* Michael Denis Mifsud (Michael.d.mifsud.10@um.edu.mt)

7 **Keywords:** Measure Correlate Predict, Wake Model, Offshore Wind Farms, LiDAR

8 Abstract

9 *This paper investigates the uncertainties resulting from different Measure-Correlate-Predict methods*
10 *to project the power and energy yield from a wind farm. The analysis is based on a case study that*
11 *utilizes short-term data acquired from a LiDAR wind measurement system deployed at a coastal site in*
12 *the northern part of the island of Malta and long-term measurements from the island's international*
13 *airport. The wind speed at the candidate site is measured by means of a LiDAR system. The predicted*
14 *power output for a hypothetical offshore wind farm from the various MCP methodologies is compared*
15 *to the actual power output obtained directly from the input of LiDAR data to establish which MCP*
16 *methodology best predicts the power generated.*

17 *The power output from the wind farm is predicted by inputting wind speed and direction derived from*
18 *the different MCP methods into windPRO®¹. The predicted power is compared to the power output*
19 *generated from the actual wind and direction data by using the Mean Squared Error (MSE) and the*
20 *Mean Absolute Error (MAE) measures. This methodology will establish which combination of MCP*
21 *methodology and wind farm configuration will have the least prediction error.*

22 *The best MCP methodology which combines prediction of wind speed and wind direction, together with*
23 *the topology of the wind farm, is that using Artificial Neural Networks. However, the study concludes*
24 *that the other MCP methodologies cannot be discarded as it is always best to compare different*
25 *combinations of MCP methodologies for wind speed and wind direction, together with different wake*
26 *models and wind farm topologies.*

27 **1 Introduction**

28 The Measure-Correlate-Predict (MCP) methodology introduces uncertainty due to its inherent
29 statistical nature. Recent developments have seen the introduction of new computational regression
30 techniques such as Artificial Neural Networks (ANN) and Machine Learning, which include Decision
31 Trees (DT) and Support Vector Regression (SVR). In a previous study, Light Detection and Ranging
32 (LiDAR) data was used to compare the results of the various regression methodologies at different
33 LiDAR measurement heights (Mifsud, et al., 2018) with the reference site being Malta International
34 Airport (MIA), Luqa, and the candidate site being a coastal watch tower at Qalet Marku on the Northern
35 part of the island. This study uses the same wind data for the year 2016 to construct the MCP models.
36 However, this time the prediction is carried out on both wind speed and wind direction. Wind speed
37 and direction are then predicted for the period June – December 2015. This is done for the different
38 MCP models. The predicted wind speed and wind direction time series are then fed into a wind farm
39 model implemented in windPRO® Ver. 2.7 to model the overall energy yield, considering wake losses.
40 The power output for various wind farm configurations is obtained for each methodology. **The LiDAR**
41 **measurements at 80m are used, since this would be equivalent to a wind turbine (WT) hub height of**
42 **100m.**

43 The power output in each case is compared to that obtained when the actual wind data is fed to the wind
44 farm model. Thus residuals, the Mean Squared Error (MSE), the Mean Absolute Error (MAE) and the
45 percentage error in the overall energy yield are compared for the various methodologies and wind farm

¹ <https://www.emd.dk/windpro>.



46 topologies. This is therefore a study about the uncertainties introduced by the various statistical
47 methods, which is then further complicated by the windfarm layout. It is innovative due to the use of
48 an MCP methodology to predict both the wind speed and the wind direction. The following literature
49 review describes different MCP methodologies, four of which are then used in the prediction of wind
50 speed and wind direction. The wake models are also described. This is followed by a description of the
51 methodology used in the study, together with a description of the hypothetical wind farm used as a basis
52 for this study. Finally, the results are presented and discussed.

53 2. Literature Review

54 The first MCP methods estimated the mean long-term annual wind speed (Carta, et al., 2013). MCP
55 methods later made use of Simple Linear Regression (SLR) (Rogers, et al., 2005) to establish a
56 relationship between hourly wind characteristics of the candidate and the reference sites. More recent
57 models established non-linear type relationships (Clive, 2004; Carta & Velazquez, 2011) by employing
58 statistical learning (Hastie, et al., 2009). Amongst these are algorithms such as Artificial Neural
59 Networks (ANNs) (Bilgili, et al., 2007; Monfared, et al., 2009) and the more recent Machine Learning
60 (ML) techniques, which include Support Vector Regression (SVR) (Oztopal, 2006; Zhao, et al., 2010;
61 Scholkopf & Smola, 2002; Alpaydin, 2010) and Decision Trees (DTs) (James, et al., 2015; Alpaydin,
62 2010).

63 A study (Carta, et al., 2013) reviewed many MCP methodologies. These included the method of ratios,
64 first-order linear regression, higher than first-order linear methods, non-linear methods and probabilistic
65 methods. The authors were also concerned with the uncertainties associated with MCP methodologies
66 and argued that users of MCP methodologies have little information on which to determine the
67 uncertainty of the methodology. One methodology to measure this uncertainty is to use the full set of
68 data from the concurrent period to train the model and assess its quality.

69 Another study by Rogers compared four different MCP methodologies (Rogers, et al., 2005). These
70 included a linear regression model, the distributions of ratios of the wind speeds at the two sites, an
71 SVR model and another method based on the ratio of the standard deviations of the two data sets. The
72 authors concluded that SVR gave the best results. In a different study, the same authors (Rogers, et al.,
73 2005b) also analysed the uncertainties introduced with the use of MCP techniques. They concluded that
74 linear regression methodologies could seriously underestimate uncertainties due to serial correlation of
75 data. Another study shows that a proper assessment of uncertainty is critical for judging the feasibility
76 and risk of a potential wind farm development, and the authors describe the risk of oversimplifying and
77 assuming uncertainties (Lackner, et al., 2012).

78 A hybrid MCP method (Zhang, et al., 2014) which involved adding different weights depending on the
79 distance and elevation of the candidate site to the reference sites, was applied to the input of five MCP
80 methodologies. The methods used consisted of the Linear Regression, Variance Ratio, Weibull scale,
81 ANNs and SVR methods. The results were assessed in terms of metrics such as the MSE and MAE.
82 Other authors (Perea, et al., 2011) evaluated three methodologies. One method included a linear
83 regression, which was derived from the bivariate normal joint distribution and the Weibull regression
84 method. The other method was based on conditional probability density functions applied to the joint
85 distributions of the reference and the candidate sites. The results from these two methodologies were in
86 turn compared to SVR. Although the conclusion was that the SVR method predicted all the parameters
87 very accurately, the probability density function based on the Weibull distribution was better in terms
88 of prediction accuracy.

89 The ability of ANNs to recognise patterns in complex data sets means that they can also be used to
90 correlate and predict wind speed and wind direction (Zhang, et al., 2014). A neural network contains an
91 input layer, one or more hidden layers of neurons and an output layer. A learning process updates the
92 weights of the interconnections and biases between the neurons in the various layers. The Levenberg-
93 Marquardt (Principe, et al., 2000) algorithm may be used for this purpose. The regression is performed
94 by means of feedforward networks (Alpaydin, 2010) with *multilayer perceptrons* (MLP).

95 Another study (Velazquez, et al., 2011) utilised wind speed and direction from various reference
96 stations. These were introduced into the input layer of an ANN. It was concluded that when wind



97 direction was used as an angular magnitude to the input signal, the model gave better results. Estimation
98 errors also decreased as the number of reference stations was increased. The authors concluded that
99 ANNs are superior to other methods for predicting long-term wind data.

100 The use of ANNs for long-term predictions was also investigated by Bechrakis (Bechrakis, et al., 2004)
101 using wind speed and direction measurements from just one reference station and compared these to
102 standard MCP algorithms. This resulted in an improved prediction accuracy of 5 to 12%. Unfortunately,
103 many models that use various reference stations use only the recorded wind speeds as input. The
104 topologies of the ANNs used have only a single neuron in the input layer, with the output signal being
105 the wind speed at the candidate site (Monfared, et al., 2009; Oztopal, 2006; Bilgili, et al., 2009).

106 Data from meteorological stations possessing long measurement periods provide a large amount of
107 potential inputs for MCP methods. Apart from wind speed and direction, inputs can also include other
108 climatological variables such as air temperature, relative humidity and atmospheric pressure. Hence, a
109 multivariate MCP methodology may be utilised (Patane, et al., 2011). This technique considers all the
110 inputs and extracts the maximum amount of information at the sites. Since some input variables may
111 be inter-correlated, or may not provide information about the target site wind characteristics, the
112 methodology is a two-stage process. Input variables are analysed and those that contain little or
113 redundant information about the candidate site wind characteristics are discarded, following which, a
114 multivariate regression is performed. It was concluded from the results of the tests made that the
115 methodology was more accurate than standard MCP methods, with the quality of the estimation of the
116 long-term wind resource increasing by 19%.

117 SVR is the adaptation of Support Vector Machines to the regression problem. This technique was
118 developed by Vapnik (Vapnik, 1995; Vapnik, et al., 1998) to solve classification problems. SVR
119 (Alpaydin, 2010) is popular within the renewable energy community, being a unique way to construct
120 smooth and nonlinear regression approximations (Diaz, et al., 2017). The analysis of MCP models using
121 SVR techniques shows that SVR is one of the techniques which best represents ML state-of-the-art
122 (Diaz, et al., 2017). This is not only due to its prediction capability, but also to its property of universal
123 approximation to any continuous function, and an efficient and stable algorithm that provides a unique
124 solution to the estimation problem (Diaz, et al., 2017). Different hyperparameters were used to study
125 the SVR methodology. Other studies describe how SVR may be adapted to wind speed prediction
126 (Zhao, et al., 2010).

127 Another recent study shows the importance of DTs in improving the regression results for MCP (Diaz,
128 et al., 2018). The study applied five different MCP techniques to mean hourly wind speed and direction,
129 together with air density, using the data from ten weather stations in the Canary Islands. The study
130 showed that the models using SVR and DTs provided better results than ANNs. A DT is a hierarchical
131 data structure which implements the ‘divide and conquer’ rule and it may also be applied to the
132 regression problem (Hastie, et al., 2009; Alpaydin, 2010; James, et al., 2015).

133 The use of LiDAR for wind resource assessment (Probst & Cardenas, 2010) shows a distinct advantage
134 of this method over the traditional cup and wind vane measurements. This is demonstrated by studies
135 carried out using different MCP methods such as SLR and ratio analysis. However, no analysis with
136 ANNs, DTs or SVR is carried out. A more recent study (Mifsud, et al., 2018), which utilised the same
137 data as this current study, analysed the accuracy of different MCP methodologies and their capability
138 according to LiDAR measurement height. The study concluded that the MCP accuracy depended on
139 both methodology and measurement height at the candidate site. Other studies using LiDAR at the same
140 measurement site were also carried out. These analysed the turbulent behaviour of the wind data
141 (Cordina, et al., 2017).

142 The issue of wake losses in a wind farm has been described by several authors and can be minimised
143 by optimising the layout of the wind farm (Manwell, et al., 2009). A short literature review of wake
144 models is now presented.

145 Wake models are classified into four categories (Manwell, et al., 2009) which are: Surface roughness
146 models (Bossanyi, et al., 1980), Semi-empirical models (Lissaman & Bates, 1977), (Vermeulen, 1980),
147 Eddy viscosity models (Ainslie, 1985), and Navier-Stokes solutions (Crespo & Hernandez, 1986),



148 (Crespo & Hernandez, 1993). A review of wind turbine wake models (Sanderse, n.d.), shows the effects
149 of reduced power production due to lower incident wind speed and the effect on the wind turbine rotors
150 due to increased turbulence. The author presents a number of reasons on why the focus on numerical
151 simulation is preferred to experimentation; this is mainly due to the use of Computational Fluid
152 Dynamics (CFD). One study presents the mathematical theory behind a simple wake model and that for
153 a multiple wake model (Gonzalez-Longatt, et al., 2012) while another study (Churchfield, 2013)
154 describes a hierarchy of wake models ranging from the empirical to large-eddy simulation (LES). Some
155 of the models compared include Ainslie's Model (Ainslie, 1985), Frandsen's model (Frandsen, 2005),
156 and Jensen's Model (Jensen, 1983). The Dynamic Wake **Meander** model is another method which is
157 described (Larsen, et al., 2008) and also validated (Larsen, et al., 2013) in a study carried out on the
158 Egmond ann Zee offshore wind farm. Another study (Barthelmie, et al., 2006), compares wake model
159 simulations for offshore wind farms, with the wake profiles being measured by Sonic Detection and
160 Ranging (SoDAR). In this case, the models gave a wide range of predictions and it was not possible to
161 identify a model with superior projections with respect to the measurements.

162 In some studies, it is necessary for any wake model used to be straightforward, dependent on relatively
163 few wake measurements and economic in terms of the necessary computing power. Despite their
164 relative simplicity, these models tend to give results which are in reasonable agreement with the
165 available data in the case of a single wake within a small wind farm and a simple meteorological
166 environment. In addition, a comparison of different wake models does not suggest any particular
167 difference in terms of accuracy, between the sophisticated and simplified models (Manwell, et al.,
168 2009).

169 The use of wake models can also be illustrated by considering a semi-empirical model (Katić, et al,
170 1986) that is often used for wind farm output predictions. This model attempts to characterise the energy
171 content in the flow field whilst ignoring the details of the exact nature of the flow field, which is assumed
172 to consist of an expanding wake with uniform velocity deficit that decreases with distance downstream
173 (Manwell, et al., 2009).

174 The N.Ø. Jensen (Jensen, 1983) is a simple wake model based on the assumption of a wake with a linear
175 wake cone. The results from this model are comparable to experimental results.

176 3. Theoretical Background

177 MCP methods are based on regression techniques. Regression can be performed by using SLR.
178 However, as mentioned above, several more powerful techniques exist amongst which are ANNs, SVR
179 and DT. While MCP methodologies have been developed for wind speed, they cannot be directly used
180 for predicting wind direction. Therefore, a method for predicting the wind direction is developed below.
181 This methodology is based upon a simple relationship (Bosart & Papin, 2017) between the
182 meteorological wind direction θ_{met} and the mathematical wind direction θ_{math} such that:

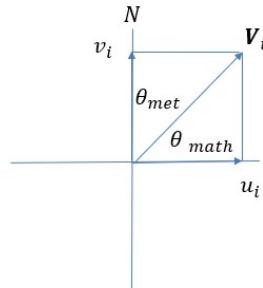
$$\theta_{math} = 90 - \theta_{met} \quad (1)$$

183 in which the wind speed vector V_i can be broken down into its vector components such that

$$u_i = |V_i| \cos \theta_{math} = |V_i| \cos(90 - \theta_{met}) \quad (2)$$

$$v_i = |V_i| \sin \theta_{math} = |V_i| \sin(90 - \theta_{met}) \quad (3)$$

184 in which case the values of u_i and v_i , which may be either positive or negative depending on the
185 direction of the wind (the value of θ_{met}), are the wind components in the North (y) and the East (x)
186 directions (axes). The relationship is shown in Figure 1.



187

188

189

Figure 1: Difference between the meteorological wind direction and the mathematical wind direction and the component of the wind vector.

190 Also,

$$|V_i| = (u_i^2 + v_i^2)^{\frac{1}{2}} \quad (4)$$

191

192

193

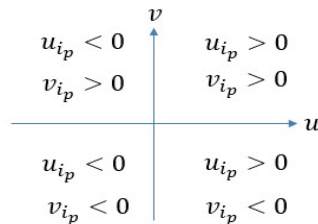
194

The regression is carried out between the respective components of the wind velocity in the y and x directions, hence establishing a relationship between the components at both sites. The forecasted wind direction at the candidate site is then obtained from the forecasted wind components using the relationship in Eq. (5):

$$\theta_{met_{i_p}} = 90 - \tan^{-1} \frac{v_{i_p}}{u_{i_p}} \quad (5)$$

195

The value of the angle $\theta_{met_{i_p}}$ depends on the direction of u_{i_p} and v_{i_p} , as shown in Figure 2



196

197

Figure 2: Calculating the value of $\theta_{met_{i_p}}$ according to the value of u_{i_p} and v_{i_p} .

198

and in accordance with the relationships shown in Eq. (6):

$$\begin{aligned} u_{i_p} > 0 \text{ and } v_{i_p} > 0 \text{ NE winds } & 0^\circ < \theta_{met_{i_p}} < 90^\circ \\ u_{i_p} > 0 \text{ and } v_{i_p} < 0 \text{ SE winds } & 90^\circ < \theta_{met_{i_p}} < 180^\circ \\ u_{i_p} < 0 \text{ and } v_{i_p} < 0 \text{ SW winds } & 180^\circ < \theta_{met_{i_p}} < 270^\circ \\ u_{i_p} < 0 \text{ and } v_{i_p} > 0 \text{ NW winds } & 270^\circ < \theta_{met_{i_p}} < 360^\circ \end{aligned} \quad (6)$$

199

and Eq. (7):



$$\begin{aligned} u_{i_p} = 0 \text{ and } v_{i_p} > 0 \text{ (North Wind)} \quad \theta_{met_{i_p}} &= 0^\circ \\ u_{i_p} = 0 \text{ and } v_{i_p} < 0 \text{ (South Wind)} \quad \theta_{met_{i_p}} &= 180^\circ \\ u_{i_p} > 0 \text{ and } v_{i_p} = 0 \text{ (East Wind)} \quad \theta_{met_{i_p}} &= 90^\circ \\ u_{i_p} < 0 \text{ and } v_{i_p} = 0 \text{ (West Wind)} \quad \theta_{met_{i_p}} &= 270^\circ \end{aligned} \quad (7)$$

200 4. A Case Study - Site Conditions and the Modelled Offshore Windfarm

201 4.1 The reference and candidate sites

202 The reference site employed in this study is the Meteorological Office at Malta International Airport
203 (MIA), Luqa, and the candidate site is data collected by a ZephIR 300 LiDAR unit administered by the
204 University's Institute for Sustainable Energy. The unit was situated on the roof of a coastal watch tower
205 at Qalet Marku, situated in the Northern Part of the Island of Malta (Mifsud, et al., 2018). The relative
206 location of the two sites is shown in Figure 3, while Figure 4 shows a satellite image of the location of
207 the coastal watch tower.



208

209 *Figure 3: Map of Malta showing relative location of the candidate and the reference sites (Google,*
210 *2019) (© Google Maps 2019).*



211

212 *Figure 4: Satellite imagery of the Qalet Marku coastal watch tower, located on a promontory near*
213 *Bahar ic-Caghaq (Google, 2019) (© Google Maps 2019).*

214 Table 1 and Table 2 show the properties of the candidate and the reference sites respectively (Cordina,
215 et al., 2017), (Mifsud, et al., 2018). In this case the wind data measured by the LiDAR at a height of
216 80m, would be equivalent to a cumulative height of 100m above sea-level, which would be the hub
217 height of the wind turbines in the windfarm as shown in Table 3.



218

Table 1: Candidate Site parameters (Cordina, et al., 2017).

Station Name	Qalet Marku LiDAR Station
Cone Angle, LiDAR aperture height above the tower rooftop.	60°, 1 m
Measurement height, above the aperture window, m	80m
Data	Hourly data
Data range	1 st July, 2015 – 31 st December, 2016
Geographical Coordinates	35.946252°N, 14.45329°E
Average tower rooftop height above surrounding ground level	10 m
Height of base of tower above sea level	6 m

219

220

Table 2: Reference Site parameters (Malta International Airport).

Station Name	Luqa MIA Weather Station
Data	Average hourly wind speed data, wind direction, air temperature, atmospheric pressure and relative humidity.
Mast height	10 m above ground
Height of site above sea level	78 m
Geographical Coordinates	35.85657°N, 14.47676°E

221 4.2 The Available Wind Data

222 The measurement campaign at the candidate site started on the 1st July 2015 and ended on the 31st
 223 December 2016. Hourly wind data were available for this time period from both the reference and
 224 candidate sites. The MCP analysis was carried out using both wind speed and wind direction. The data
 225 from the reference site were used as the independent data set. The models were created using the data
 226 for the year 2016, while the reference site wind data for 2015 used to create the predicted wind speed
 227 and wind direction as inputs to the windfarm model.

228 4.3 The Wind Farm Design in windPRO®

229

Table 3: Wind Turbine Parameters used in the study (wind-turbine-models.com, 2019).

Wind Turbine Parameter	
Manufacturer	RE Power (Germany)
Rated Power	5000 W
Rotor orientation	Upwind
Number of blades	3
Rotor Diameter	126 m
Swept Area	12469 m ²
Blade Type	LM
Cut in speed	3.5 ms ⁻¹
Rated Wind Speed	14 ms ⁻¹
Cut out speed (for off-shore)	30 ms ⁻¹
Hub-height, z	100 m

230 The hypothetical wind farm is located opposite the coastal watch tower of Qalet Marku [14.452498°E,
 231 35.945892°N]. windPRO® 2.7 was used to render an image of the wind farm onto an image of the
 232 LiDAR unit taken from the watch tower. This gives an indication as to the extent of the wind farm. This
 233 is shown in Figure 5, while Figure 6 shows the satellite imagery of the wind farm, showing a 250-MW



234 capacity windfarm. The windfarm faces the North-West direction, which is the prevailing wind
235 direction.

236 The wind turbines are located at a distance of five rotor diameters ($5D$) from each other while the
237 distance between the rows of the wind turbines is eight diameters ($8D$). Hence, considering wind
238 turbines with a rotor diameter, D , of 126 m (for a 5 MW Wind Turbine), the distance between the
239 turbines in the cross-wind direction is 630 m , and the distance between successive rows of wind
240 turbines in the downwind direction is $1,008\text{ m}$. The wind turbine selected for use in windPRO® is the
241 RE Power 5-MW wind turbine whose parameters are shown in Table 3.



242
243

Figure 5: View of the wind farm rendered onto an image of the area and also showing the LiDAR unit.



244
245
246

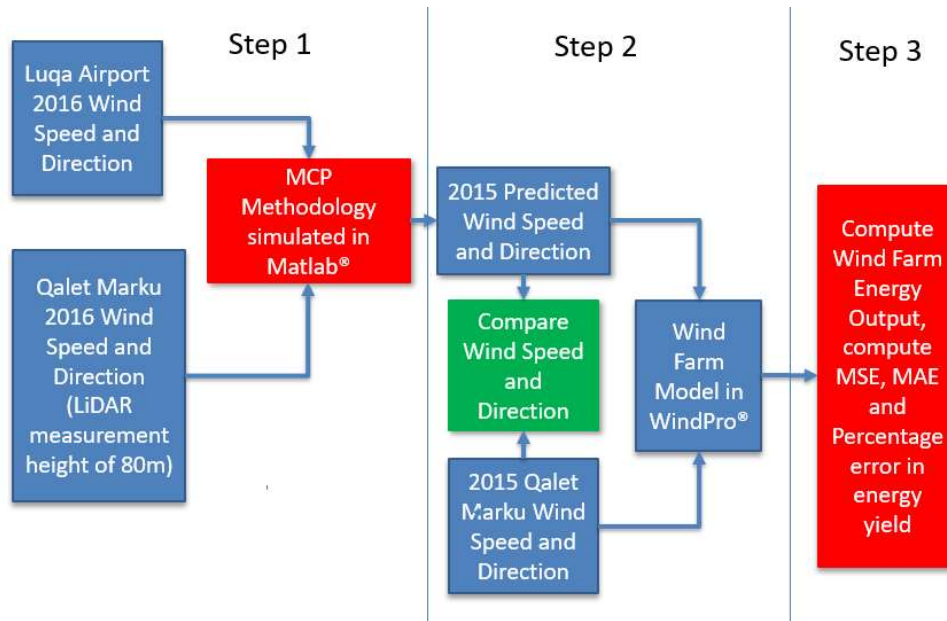
Figure 6: Satellite imagery of the wind farm showing the location of the 50 wind turbines with respect to the coastal LiDAR station (Google, 2019) (© Google Maps 2019).

247 5. Methodology

248 Figure 7 shows the methodology applied in this paper:



249



250

251

Figure 7: Applied methodology.

252 The study is divided into three steps as follows:

- 253 1. STEP 1 - The various MCP methodologies are used to compute the MCP model. This is done using
- 254 wind speed and direction data at a candidate and reference site for the year 2016.
- 255 2. STEP 2 - The 2015 wind speed and wind direction are predicted using the models computed in
- 256 Step 1. The predicted and actual wind speed and wind direction are used to compute the power
- 257 output from the wind farm. This is done by feeding the wind speed and direction data into the
- 258 windPRO® model, and,
- 259 3. STEP 3 - compute and compare the MSE, MAE and percentage error in the power.

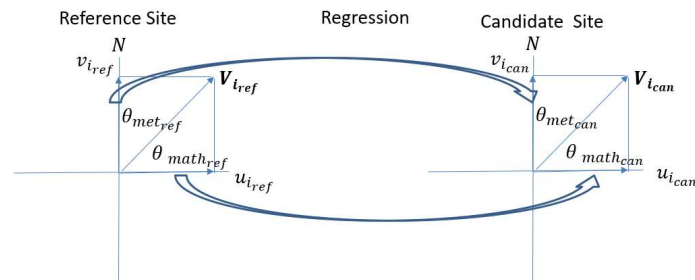
260 The combinations of LiDAR measurement heights and MCP methodologies are shown in Table 4.

261 Table 4: Summary of combinations of methodologies, LiDAR measurement heights and amount of wind turbines used in the
 262 analysis

80m (equivalent to a 100m hub height)	MCP Methodology			
	Simple Linear Regression (SLR)	Artificial Neural Networks (ANN)	Decision Trees (DT)	Support Vector Regression (SVR).
	Wind Speed, Wind Direction, predicted for 2015. Actual and predicted sequences fed into wind farm model, comparisons of wind farm power output made for a capacity of 250, 200, 150, 100 and 50 MW.			

263 Regression models were created for the MCP methodologies using the reference and candidate wind
 264 speed and direction for the year 2016. These regression models were created using SLR, ANN, DT and
 265 SVR. A model was created for both wind speed and direction.

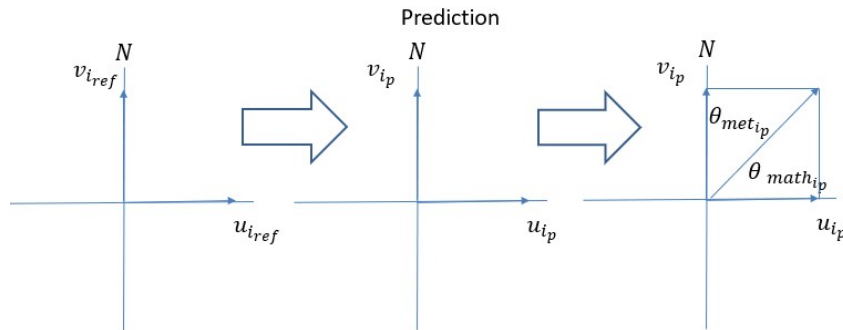
266 The wind speed and wind direction for 2015 were then predicted with the models by feeding the speed
 267 and direction values from the reference site from the year 2015. Thus, a sequence of predicted wind
 268 speeds and wind direction time series could be compared to the actual speed and direction measured at
 269 the candidate site for the year 2015. The models for the wind speed and the wind direction are
 270 independent from each other.



271
 272

Figure 8: Application of regression methodologies to wind direction

273 In the case of wind direction, the MCP methodologies are applied as shown in Figure 8 and Figure 9.
 274 Figure 8 shows that two regressions are carried out: one for the magnitude of the wind component in the
 275 North direction and one for the wind component in the East direction. Thus, two models are created
 276 using the wind speed and direction data of the reference and the candidate site for 2016. The two models
 277 are then used to derive the predicted wind direction for 2015 at the candidate site as shown in Figure 9,
 278 by using the wind components at the reference site for 2015 as inputs to the respective models. The
 279 values of the wind speed in the North direction and the East direction are first predicted, and the wind
 280 direction at the candidate site for 2015, θ_{met_p} , is then derived from the mathematical relationships given
 281 in Eq. (6) and Eq. (7).



282
 283

Figure 9: Predicting the wind direction

284 The sequences of wind speed and wind directions (both actual and predicted) were fed into the wind
 285 farm model. This was done for different combinations of methodology and wind farm (250, 200, 150,
 286 100 and 50 MW) configurations. The results were compared to determine which combination of MCP
 287 methodology, and windfarm capacity would give the lowest prediction error. The prediction error for
 288 the power output from the wind farm is analysed using the Mean Squared Error (MSE), the Mean
 289 Absolute Error (MAE) and the percentage error in the Overall Energy Yield for the period of analysis.
 290 The results are shown in the following section.

291 6. Results

292 A summary of the results is shown below where sequences of data for a specific period of 2015 are
 293 compared. These sequences are for wind speed, wind direction and power output. All MSE, MAE and
 294 percentage errors in the overall energy yield are then shown in the following tables.

295 6.1 Wind speed and wind direction with MCP methodology.

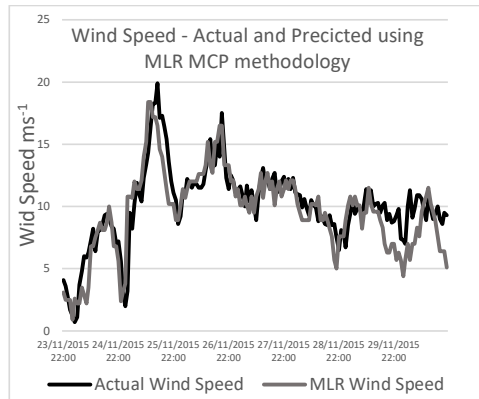
296 6.1.1 Wind speed with MCP methodology.

297 Figure 10 to Figure 13 show the wind speed from the period 23rd November to the 30th November 2015.
 298 The particular period is chosen because of the high availability of wind. The actual wind data are



299 compared with that predicted by the MLR, ANN, DT and SVR methodologies. The predicted wind
300 values closely follow the actual wind values, for all the MCP methodologies applied.

301



302
303
304 *Figure 10: Comparing actual wind speed and wind speed predicted by MLR methodology with wind data for 2015.*

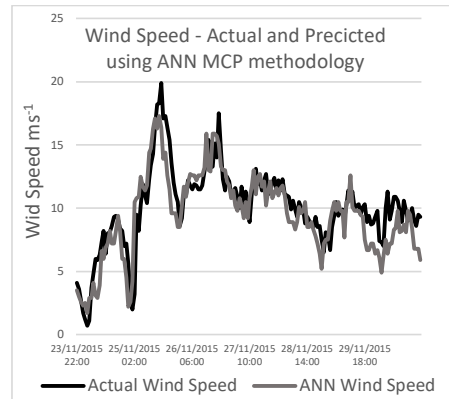
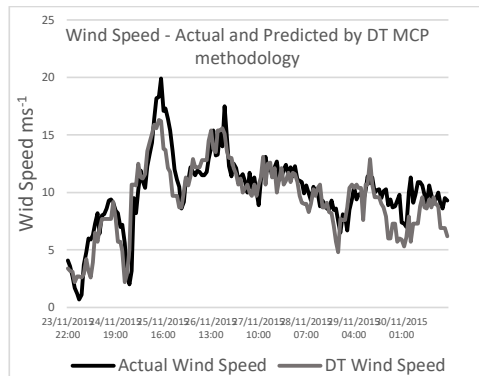


Figure 11: Comparing actual wind speed and wind speed predicted by ANN methodology with wind data for 2015.



308
309
310 *Figure 12: Comparing actual wind speed and wind speed predicted by DT methodology with wind data for 2015.*

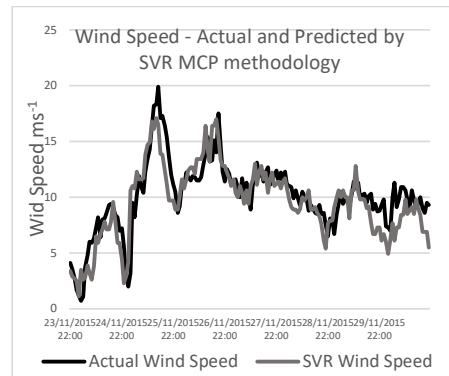
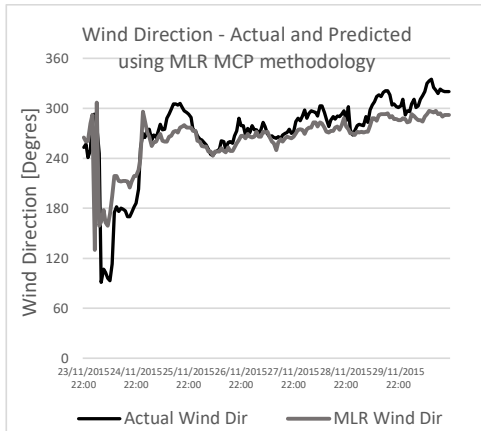


Figure 13: Comparing actual wind speed and wind speed predicted by SVR methodology with wind data for 2015.

314 6.1.2 Wind direction with MCP methodology.

315 Figure 14 to Figure 17 show the wind direction from the period 23rd November to the 30th November
316 2015. As above, the actual wind direction at the candidate site is compared to that predicted by the
317 MLR, ANN, DT and SVR methodologies. Again, as in the case for wind speed, there is a similarity
318 between the actual and predicted wind direction values, in all cases.

319



320
321
322 *Figure 14: Comparing actual and predicted wind direction predicted by MLR methodology, with wind data for 2015.*

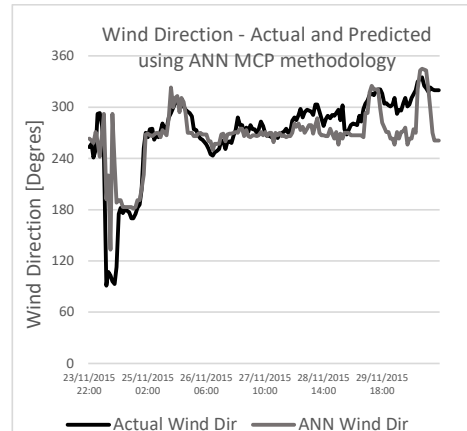
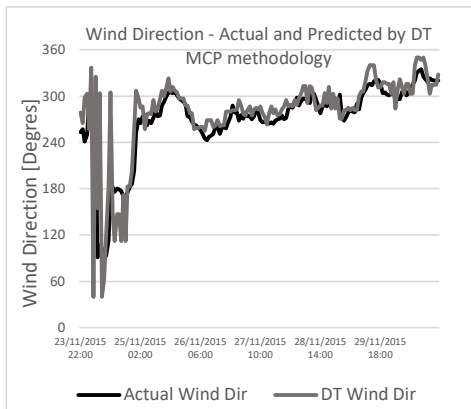


Figure 15: Comparing actual and predicted wind direction predicted by ANN methodology, with wind data for 2015.

326



327
328
329 *Figure 16: Comparing actual and predicted wind direction predicted by DT methodology, with wind data for 2015.*

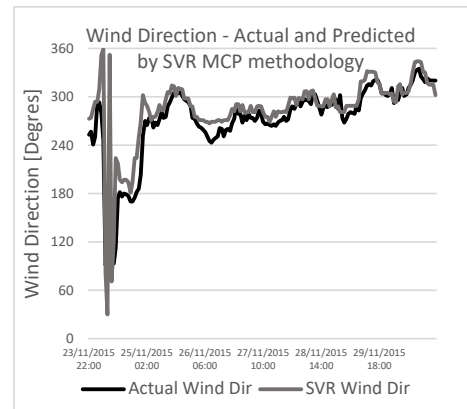
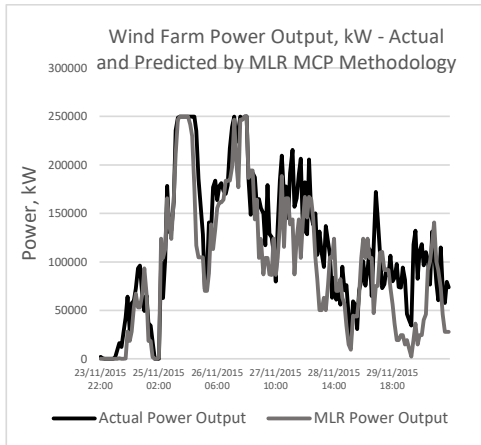


Figure 17: Comparing actual and predicted wind direction predicted by SVR methodology, with wind data for 2015.

333 **6.2 Wind farm power output with MCP methodology, for a windfarm capacity of**
334 **250MW.**

335 Figure 18 to Figure 21 compare the output power from the wind farm, which is derived from the actual
336 wind speed and wind direction to the power output derived from the predicted wind speed and direction.
337 This comparison is carried out for the MLR, ANN, DT and SVR methodologies. The results for a wind
338 farm capacity of 250MW are being shown. As in the case for wind speed and direction, the predicted
339 power output closely follows that obtained with the actual wind speed and direction.

340



341
342 *Figure 18: Comparing actual and predicted power output*
343 *from the wind farm, with wind data for 2015, actual and*
344 *predicted by MLR methodology.* 348

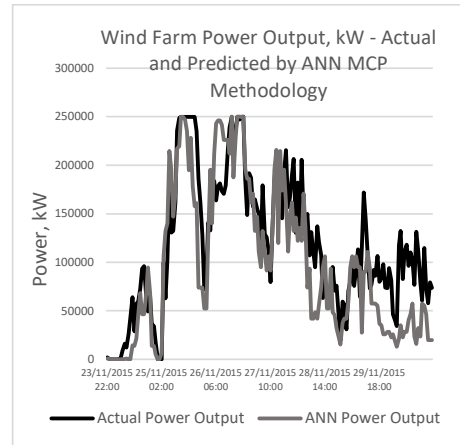
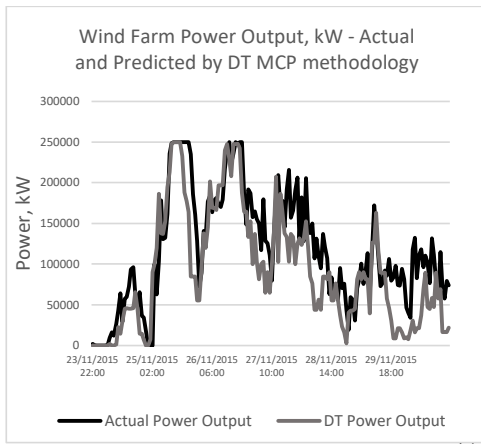


Figure 19: Comparing actual and predicted power output
from the wind farm, with wind data for 2015, actual and
predicted by ANN methodology.



349
350 *Figure 20: Comparing actual and predicted power output*
351 *from the wind farm, with wind data for 2015, actual and*
352 *predicted by DT methodology.* 356

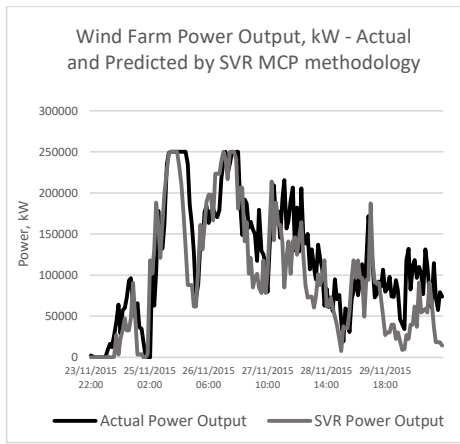


Figure 21: Comparing actual and predicted power output
from the wind farm, with wind data for 2015, actual and
that predicted by SVR methodology.

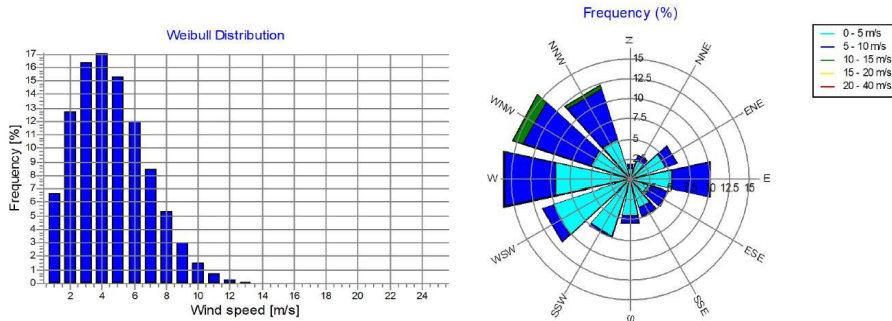
357

358 A Wind Data Analysis, carried out using windPRO®, is shown in the next section. The results presented
359 are a Weibull distribution for wind speed and the wind rose. These charts are computed from the wind
360 speed and direction which are predicted by using the MLR, ANN, DT and SVR MCP methodologies.
361 Thus, the predicted wind speed and direction are compared with the results computed from the actual
362 wind data.

363 6.3 The Actual Wind Data for 2015 measured by the LiDAR system.

364 Figure 22 shows the Wind Data Analysis report from windPRO® for the actual LiDAR data measured
365 at the 80m level height (equivalent to a hub height of 100m). The images show the Weibull distribution
366 for the wind speed and the wind rose. The reports are used to compare the properties of the actual wind
367 measurements and the predicted wind speed and direction.

368



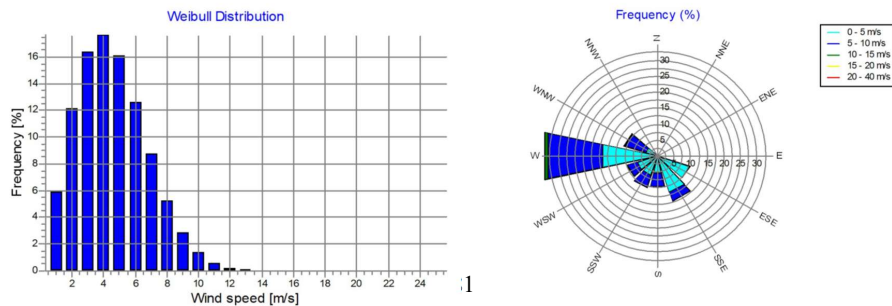
369

370 *Figure 22: windPRO® wind data analysis using actual wind data measured by the LiDAR equipment at a height of 100 m.*

371 **6.4 Wind speed and direction predicted using the MCP methodologies.**

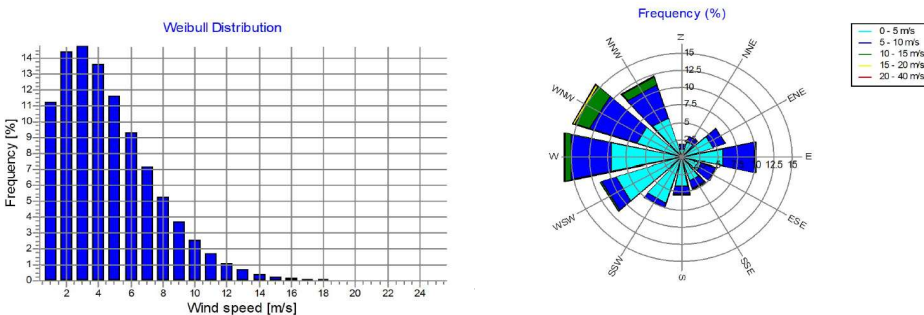
372 Figure 23 to Figure 26 represent the Weibull distribution and the wind rose for the wind speed and
 373 direction predicted by the MLR, ANN, DT and SVR MCP methodologies respectively, at the hub height
 374 of 100m. There exists a similarity between the Weibull plots for the actual wind data and those for the
 375 predicted wind speed, for the same measurement period. While, the wind direction predicted by the
 376 ANN and DT methodologies show a higher resemblance to that of the actual wind direction than that
 377 predicted by the MLR or SVR methodologies. Hence it is expected that the ANN and the DT
 378 methodologies would yield the least error in the predicted power output from the wind farm.

379



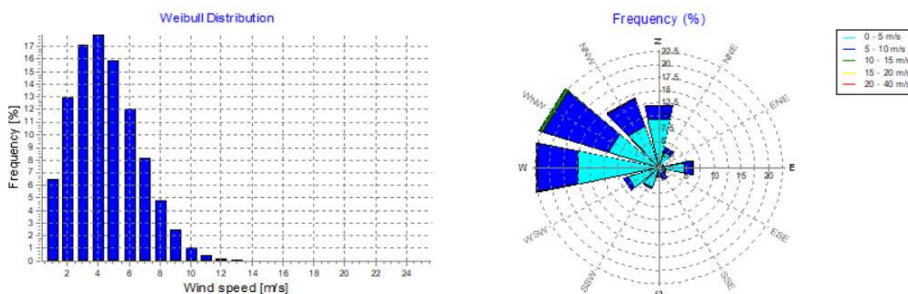
380

382 *Figure 23: windPRO® wind data analysis using wind data predicted by MCP applying MLR at a hub height of 100 m.*



383

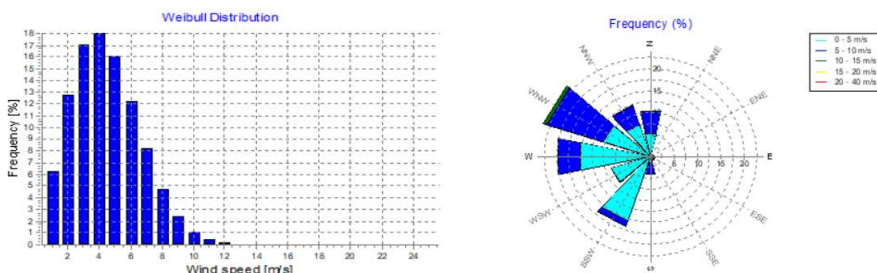
385 *Figure 24: windPRO® wind data analysis using wind data predicted by MCP applying ANN at a hub height of 100 m.*



386

387

388 *Figure 25: windPRO® wind data analysis using wind data predicted by MCP applying DT at a hub height of 100 m*



389

391 *Figure 26: windPRO® wind data analysis using wind data predicted by MCP applying SVR at a hub height of 100 m*

392 The results for the MAE, the MSE and the percentage error in the Overall Energy Yield are summarised
 393 in Table 5 to Table 7. The tables show that the DT and ANN methodology have the best performance
 394 in MAE and MSE. While MLR and ANN have the best performance in percentage error in energy yield.
 395 The results are consistent for all wind farm capacities under consideration, with the error decreasing
 396 with decreasing wind farm capacity. The decrease in error is expected, as in this case the uncertainty
 397 due to the wake losses is reduced, when the wind blows from the prevailing direction, especially in the
 398 case of the lower wind farm capacities.

399 *Table 5: Summarised results for Mean Absolute Error by MCP methodology and windfarm capacity.*

Mean Absolute Error [kW]				
Wind Farm Capacity	MLR	ANN	DT	SVR
250MW	10,999	10,850	10,590	11,197
200MW	8,944	8,801	8,608	9,108
150MW	6,851	6,733	6,598	6,979
100MW	4,687	4,612	4,525	4,764
50MW	2,455	2,397	2,364	2,462

400

401



402

Table 6: Summarised results for the Mean Squared Error by MCP methodology and windfarm capacity.

Mean Squared Error [MW] ²				
Wind Farm Capacity	MLR	ANN	DT	SVR
250MW	491.07	479.96	476.34	499.51
200MW	320.69	311.75	308.23	326.09
150MW	184.12	178.96	176.00	187.29
100MW	82.77	81.19	79.27	84.53
50MW	21.33	20.95	20.65	21.40

403

404

Table 7: Summarised results for percentage error in overall energy yield by MCP methodology and windfarm capacity.

Percentage Error in Overall Energy Yield				
Wind Farm Capacity	MLR	ANN	DT	SVR
250MW	4.63	4.54	18.83	9.44
200MW	4.80	4.90	18.40	9.34
150MW	4.92	5.40	17.78	9.23
100MW	4.78	5.70	16.92	8.71
50MW	3.65	7.03	14.73	8.23

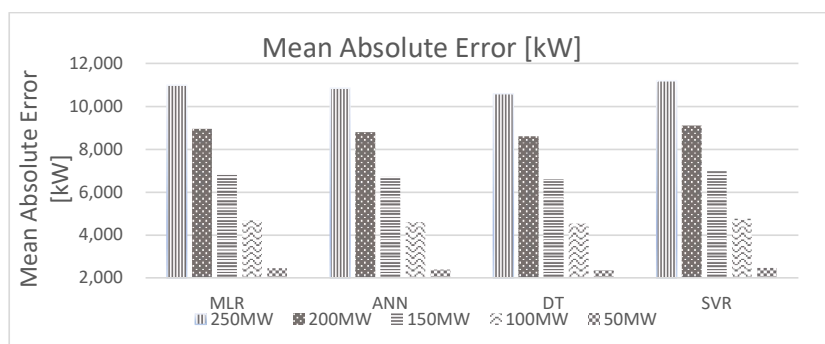
405

406

407

408

Results are also shown in Figure 27 to Figure 29, which show a slight superiority of the DT methodology in terms of MAE and MSE, and a net superiority of the MLR and ANN methodologies in the percentage error of the overall energy yield.

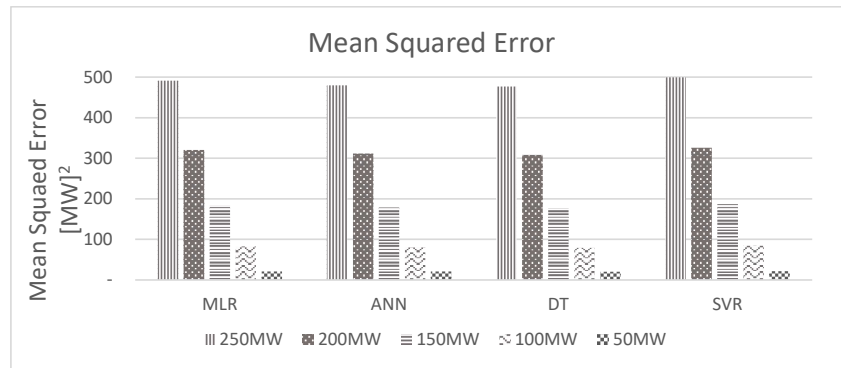


409

410

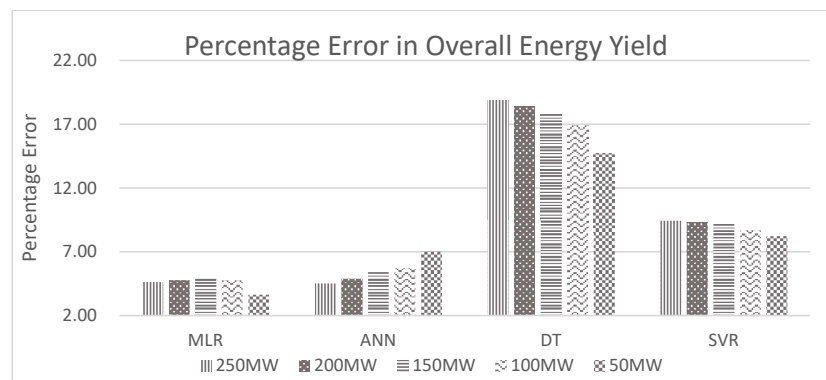
411

Figure 27: Comparison of the Mean Absolute Error for the various wind farm topologies and MCP methodology, for the 2015 energy output from the wind farm.



412
 413
 414

Figure 28: Comparison of the Mean Standard Error for the various wind farm topologies and MCP methodology, for the 2015 energy output from the wind farm.



415
 416
 417

Figure 29: Comparison of the Percentage Error in Overall Energy Yield for the various wind farm topologies and MCP methodology, for the 2015 energy output from the wind farm.

418 When considering the MAE and the MSE, the differences between the DT and the ANN methodologies
 419 are minimal and the DT performs better. However, the ANN methodology shows a much better
 420 performance than the DT methodology, in the percentage error in the energy yield from the wind farm.
 421 The ANN methodology also shows the best similarity to the actual wind speed and wind direction, as
 422 seen in Figure 24. Although the MLR methodology shows a significant improvement in percentage
 423 error, it is only slightly better than the ANN methodology, for the 250MW and 200MW windfarm
 424 capacity. The MLR methodology has better results in the case of 150MW, 100MW and 50MW wind
 425 farm capacities, with the percentage error being 3.5% at a windfarm capacity of 50MW, when
 426 compared to an error of 7.3% obtained with the ANN methodology. The MLR methodology is inferior
 427 to the ANN or DT methodologies, in the case of MAE and MSE. Thus, it may be concluded that the
 428 ANN approach is the best MCP methodology for predicting the energy yield for the offshore windfarm.
 429 The SVR methodology has the worst overall performance.

430 7. Conclusions

431 The above research has combined the use of MCP methodologies for wind speed and used a different
 432 method for predicting the wind direction at a candidate site. Three of the four MCP methodologies used
 433 are based on modern statistical learning methodologies. The data was collected from a reference site
 434 which is the Island of Malta's international airport, while the candidate site data has been collected by
 435 means of a LiDAR wind measurement system placed on the roof top of a coastal building.

436 The wind direction at the candidate site was predicted with the various MCP methodologies by breaking
 437 down the wind velocity vector into its respective North and East direction components. The regression



438 analysis was then carried out on the respective components at the reference and the candidate sites. The
439 wind speed is predicted by using the magnitude of the wind speed at the respective sites for creating the
440 regression model.

441 The projected wind speed and direction time series were applied to a hypothetical wind farm. Thus, the
442 error introduced by the four MCP methods could be measured. This was done by calculating the MSE, the
443 MAE and the percentage error in wind farm's energy yield. The results show that the MSE, MAE
444 and the percentage error in energy yield depend on the MCP methodology and the windfarm capacity.

445 In this case, the best MCP method was that which used Artificial Neural Networks. Although other
446 MCP methodologies gave larger errors, they cannot be totally discarded. It is always best to compare
447 methodologies, comparing results by analysing residuals and errors and then choosing the best
448 methodology on a case-by-case basis.

449 Unless actual wind data is available, one cannot carry out this analysis, as the uncertainty is obtained
450 by comparing the energy from the windfarm with predicted and actual wind data. The above analysis
451 could be done because 18 months of data were available, rather than the normal 12 months, which is
452 usual for a wind resource assessment which uses MCP methodologies.

453 The above study was limited to using the same MCP methodology for both the wind speed and direction
454 and to the N.Ø. Jansen methodology for wake losses. The layout chosen was one that ensured a
455 recommended minimum distance between the wind turbines. Different combinations of MCP
456 methodologies for wind speed and direction can be examined. For example, the combination of the
457 ANN methodology to predict wind speed and SVR for wind direction or vice-versa. This is an area
458 which warrants further study, as is trying out different windfarm topologies, or selecting different wind
459 turbines. It would also be of interest to study the application of different wake methodologies as a
460 possible means of decreasing the uncertainties.

461 **8. Author Contribution.**

462 Tonio Sant and Robert.N.Farrugia contributed in the preparation of the manuscript and the research
463 methodology.

464 **9. Competing Interests.**

465 The authors declare that they have no conflict of interest.

466 **10. Acknowledgements.**

467• Mr. Joseph Schiavone from the Meteorological Office at Malta International Airport, Luqa, is being
468 acknowledged for providing the data for the Luqa MIA Weather Station.

469• The authors would like to express their sincere gratitude to Mr. Manuel Aquilina, lab officer at the
470 University of Malta, for technical assistance in collecting and organising the data from the Institute for
471 Sustainable Energy's LiDAR system at Qalet Marku.

472• The LiDAR system was purchased through the European Regional Development Fund (ERDF 335),
473 part-financed by the European Union.

474• Thanks also goes to Din L'Art Helwa for permitting and facilitating the installation of the LiDAR unit
475 on the Qalet Marku Tower.

476• The windPRO® 2.7 software was funded by the project: *Setting up of Mechanical Engineering*
477 *Computer Modelling and Simulation Laboratory*, part-financed by the European Regional Development
478 Fund (ERDF) - Investing in Competitiveness for a Better Quality of Life, Malta 2007 – 2013.

479 **11. Nomenclature.**

480	ANN	Artificial Neural Network
481	CFD	Computational Fluid Dynamics
482	DT	Decision Trees
483	LiDAR	Light Detection and Ranging



484	LSE	Large Eddy Simulation
485	MIA	Malta International Airport
486	MAE	Mean Absolute Error
487	MCP	Measure-Correlate-Predict
488	MLP	Multilayer Perceptron
489	MSE	Mean Squared Error
490	SLR	Simple Linear Regression
491	SoDAR	Sonic Detection and Ranging
492	SVR	Support Vector Regression
493	WT	Wind Turbine
494		
495	V_i	Magnitude of wind speed in ms^{-1}
496	u_{ip}	Predicted component of wind speed vector in easterly direction at the candidate site in ms^{-1}
497		
498	$u_{i_{ref}}$	Component of wind speed vector in easterly direction at the reference site in ms^{-1}
499		
500	$u_{i_{ref}}$	Component of wind speed vector in easterly direction at the reference site in ms^{-1}
501		
502	u_i	Component of wind speed vector in easterly direction in ms^{-1}
503	$v_{i_{can}}$	Component of wind speed vector in northerly direction at the candidate site in ms^{-1}
504		
505	v_{ip}	Predicted component of wind speed vector in northerly direction at the candidate site in ms^{-1}
506		
507	$v_{i_{ref}}$	Component of wind speed vector in northerly direction at the reference site in ms^{-1}
508		
509	v_i	Component of wind speed vector in northerly direction in ms^{-1}
510	z_0	surface roughness
511	V_i	Wind speed vector (speed in ms^{-1} , wind direction in deg)
512	$\theta_{math_{ip}}$	Predicted mathematical wind direction at the candidate site in deg
513	$\theta_{met_{ip}}$	Predicted meteorological wind direction at the reference site in deg
514	$\theta_{met_{can}}$	Meteorological wind direction at the candidate site in deg
515	$\theta_{met_{ref}}$	Meteorological wind direction at the reference site in deg
516	θ_{math}	Mathematical wind direction
517	θ_{met}	Meteorological wind direction
518	D	Wind turbine diameter, m

519

520 **12 References.**

521 Ainslie, J., 1985. Calculating the Flowfield in the Wake of Turbines. *Journal of Wind*
 522 *Engineering and Industrial Aerodynamics*, Volume 27, pp. 216 - 224.

523 Alpaydin, E., 2010. *Introduction to Machine Learning*. 2nd Edition ed. s.l.:Massachusetts
 524 Institute of Technology.

525 Barthelmie, R. et al., 2006. Comparison of Wake Model Simulations with Offshore Wind
 526 Turbine Wake Profiles Measured by Sodar. *Journal of Atmospheric and Oceanic Technology*,
 527 Volume 23, pp. 888-901.

528 Bechrakis, D., Deane, J. & MCKeogh, E., 2004. Wind Resource Assessment of an Area using
 529 Short-Term Data Correlated to a Long-Term Data-Set.. *Solar Energy*, Volume 76, pp. 724-32.



- 530 Bilgili, M., Sahin, B. & Yaser, A., 2009. Application of Artificial Neural Networks for the
531 Wind Speed Prediction of Target Station using Reference Stations Data. *Renewable Energy*,
532 Volume 34, pp. 845 - 848.
- 533 Bilgili, M., Sahlin, B. & Yasar, A., 2007. Application of Artificial Neural Networks for the
534 Wind Speed Prediction of Target Station Using Artificial Intelligent Methods. *Renewable*
535 *Energy*, Volume 32, pp. 2350-60.
- 536 Bosart, L. & Papin, P., 2017. www.atmos.albany.edu. [Online]
537 Available at: www.atmos.albany.edu/.../2017/pptx/ATM305_Statistics_16Nov17.pptx
538 [Accessed 3 March 2019].
- 539 Bossanyi, E. et al., 1980. *The Efficiency of Wind Turbine Clusters*. Lyngby, DK, s.n.
- 540 Carta, J. & Velazquez, S., 2011. A New Probabilistic Method to Estimate the Long-Term Wind
541 Speed Characteristics at a Potential Wind Energy Conversion Site. *Energy*, Volume 36, pp.
542 2671-85.
- 543 Carta, J., Velazquez, S. & Cabrera, P., 2013. A Review of Measure-Correlate-Predict (MCP)
544 methods used to Estimate Long-Term Wind Characteristics at a Target Site. *Renewable and*
545 *Sustainable Energy Reviews*, Volume 27, pp. 362-400.
- 546 Carta, J., Velazquez, S. & Matias, J., 2011. Use of Bayesian Network Classifiers for Long-
547 Term Mean Wind-Turbine Energy Output Estimation at a Potential Wind Energy Conversion
548 Site. *Energy Conversion and Management*, Volume 52, pp. 1137-49.
- 549 Churchfield, M., 2013. *A review of Wind Turbine Wake Models and Future Directions*, Boulder,
550 Colorado: National Renewable Energy Laboary.
- 551 Clive, J., 2004. Non-linearity of MCP with Weibull Distributed Wind Speeds. *Wind*
552 *Engineering*, Volume 28, pp. 213-24.
- 553 Cordina, C., Farrugia, R. & Sant, T., 2017. *Wind Profiling using LiDAR at a Costal Location*
554 *on the Mediterranean Island of Malta*. s.l., s.n.
- 555 Crespo, A. & Hernandez, J., 1986. *A Numerical Model of Wind Turbine Wakes and Wind*
556 *Farms*. Rome, s.n.
- 557 Crespo, A. & Hernandez, J., 1993. *Analytical Corelations for Turbulence Characteristics in*
558 *the Wakes of Wind Turbines*. Lubeck, s.n.
- 559 Diaz, S., Carta, J. & Matias, J., 2017. Comparison of Several Measure-Correlate-Predict
560 Models using Support Vector Regression Techniques to estimate wind power densities. A case
561 study. *Energy Conversion and Management*, Volume 140, pp. 334-354.
- 562 Diaz, S., Carta, J. & Matias, J., 2018. Performance Assessment of Five MCP Models Proposed
563 for the Estimation of Long-term Wind Turbine Power Outputs at a Target Site Using Three
564 Machine Learning Techniques. *Applied Energy*, Issue 209, pp. 455-477.
- 565 Draper, N. & Smith, H., 2015. *Applied Regression Analysis*. 3rd ed. s.l.:John Wiley and Sons,
566 Inc.
- 567 Fransden, S., 2005. *Turbulence and Turbulene-Generated Structural Loading in Wind Turbine*
568 *Clusters*, s.l.: Riso National Laboratory.
- 569 Gonzalez-Longatt, F., Wall, P. & Terzija, V., 2012. Wake effect in wind farm performance:
570 Steady State and Dynamic Behaviour. *Renewable Energy*, Volume 39, pp. 329 - 338.
- 571 Google, 2019. *Google Earth*. [Online].



- 572 Hastie, T., Tibshirani, R. & Friedman, J., 2009. *The Elements of Statistical Learning, Data*
573 *Mining, Inference and Prediction*. Second ed. New York: Springer Series in Statistics.
- 574 James, G., Witten, D., Hastie, T. & Tibshirane, R., 2015. *An Introduction to Statistical*
575 *Learning with Applications in R*. New York: Springer Texts in Statistics.
- 576 Jensen, N., 1983. *A note on Wind Generator Interaction*, s.l.: Riso National Laboratory.
- 577 Koch, F. et al., 2005. *Consideration of Wind Farm Wake Effect in Power System Dynamic*
578 *Simulation*. s.l., IEEE.
- 579 Lackner, M., Rogers, A.L., & Manwell, J., 2012. *Uncertainty Analysis in Wind Resource*
580 *Assessment and Wind Energy Production Estimation*. Reno, Nevada, American Institute of
581 Aeronautics and Astronautics, Inc..
- 582 Larsen, G., Madsen, H. A., Larsen, T. J. & Troldborg, N., 2008. *Wake Modelling and*
583 *Simulation*, s.l.: Technical University of Denmark.
- 584 Larsen, T., Madsen, H., G.C., L. & Hansen, K., 2013. Validation of the Dynamic Wake
585 Meander Model for Loads and Power Production in the Egmond aan Zee Wind Farm. *Wind*
586 *Energy*, 10 October, Volume 16, pp. 605-624.
- 587 Lissaman, P. & Bates, E., 1977. *Energy Effectiveness of Arrays of Wind Energy Conversion*
588 *Systems*, Pasadena, CA: s.n.
- 589 Manwell, J., McGowan, J. & Rogers, A., 2009. *Wind Energy Explained*. 2nd ed. s.l.: John Wiley
590 and Sons Ltd..
- 591 Marvin, L., n.d. *Neural Networks with Matlab*. s.l.: Amazon.
- 592 Mifsud, M., Sant, T. & Farrugia, R., 2018. A Comparison of Measure-Correlate-Predict
593 Methodologies using LiDAR as a Candidate Measurement Device for the Mediterranean Island
594 of Malta. *Renewable Energy*, Issue 127, pp. 947 - 959.
- 595 Monfared, M., Rastegar, H. & Kojabadi, H., 2009. A New Strategy for Wind Speed Forecasting
596 Using Artificial Intelligent Methods. *Renewable Energy*, Volume 34, pp. 845-8.
- 597 Montgomery, D., Peck, E. & Vinning, G., 2006. *Introduction to Linear Regression Analysis*.
598 s.l.: John Wiley & Sons, Inc..
- 599 Oztopal, A., 2006. Artificial Neural Network Approach to Spatial Estimation of Wind Velocity.
600 *Energy Conversion and Management*, Volume 47, pp. 395 - 406.
- 601 Patane, D. et al., 2011. *Long Term Wind Resource Assessment by means of Multivariate Cross-*
602 *Correlation Analysis*. Brussels, Belgium, s.n.
- 603 Perea, A., Amezcua, J. & Probst, O., 2011. Validation of Three New Measure-Correlate
604 Predict Models for the Long-Term Prospection of the Wind Resource. *Journal of Renewable*
605 *and Sustainable Energy*, Volume 3, pp. 1-20.
- 606 Principe, J., Euliano, N. & Curt Lefebvre, W., 2000. *Neural and Adaptive Systems:*
607 *Fundamentals Through Simulations*. s.l.: John Wiley & Sons, Inc..
- 608 Probst, O. & Cardenas, D., 2010. State of the Art and Trends in Wind Resource Assessment.
609 *Energies*, Volume 3, pp. 1087 - 1141.
- 610 Rogers, A., Rogers, J. & Manwell, J., 2005. Comparison of the Performance of four Measure-
611 Correlate-Predict Models for Long-Term Prospection of the Wind Resource. *Journal of Wind*
612 *Engineering and Industrial Aerodynamics*, 93(3), pp. 243-64.



- 613 Rogers, A., Rogers, J. & Manwell, J., 2005b. Uncertainties in Results of Measure-Relate-
614 Predict Analyses. *American Wind Energy Association*, May.
- 615 Sanderse, B., n.d. *Aerodynamics of wind turbine wakes: Literature review*, s.l.: Energy
616 Research Centre of the Netherlands.
- 617 Scholkopf, B. & Smola, A., 2002. *Learning with Kernels - Support Vector Machines,*
618 *Regularisation, Optimisation and Beyond*. Cambridge(Massachusetts): The MIT Press.
- 619 Vapnik, V., 1995. *The Nature of Statistical Learning Theory*. NY: Springer.
- 620 Vapnik, V., Golowich, S. & Smola, A., 1998. A Support Vector Method for Function
621 Approximation, Regression Estimation and Signal Processing. *Advances in Neural Information*
622 *Processing Systems*, pp. 281-7.
- 623 Velazquez, S., Carta, J. & Matias, J., 2011. Comparision between ANNs and Linear MCP
624 algorrithms in the Long-Term Estimation of the Cost per kW h Produced by a Wind Turbine
625 at a Candidate Site: A Case Study in the Canary Islands. *Applied Energy*, Volume 88, pp. 3869-
626 81.
- 627 Vermeulen, P., 1980. *An Experimental Analysis of Wind Turbine Wakes*. Lyngby, DK, s.n., pp.
628 431-450.
- 629 Vermeulen, P., Builties, P., Dekker, J. & Lammerts van Buren, G., 1979. *An Experimental*
630 *Study of the Wake Behind a Full-Sacal Vertical-Axis Wind Turbine*, s.l.: s.n.
- 631 wind-turbine-models.com, 2019. *wind-turbine-models.com*. [Online]
632 Available at: <https://en.wind-turbine-models.com/turbines/1-repower-5m-offshore>
633 [Accessed 19 March 2019].
- 634 Zhang, J., Chowdhury, S., Messac, A. & Hodge, B.-M., 2014. A Hybrid Measure-Relate-
635 Predict Method for Long-Term Wind Condition Assessment. *Energy Conversion and*
636 *Management*, Volume 87, pp. 697-710.
- 637 Zhao, P., Xia, J., Dai, Y. & He, J., 2010. *Wind Speed Prediction Using Support Vector*
638 *Regression*. Taiwan, IEEE.
- 639
640